PHYSICAL REVIEW E **76**, 035301(R) (2007)

Front fingering and complex dynamics driven by the interaction of buoyancy and diffusive instabilities

J. D'Hernoncourt,[1] J. H. Merkin,[2] and A. De Wit[1]

[1]*Nonlinear Physical Chemistry Unit and Center for Nonlinear Phenomena and Complex Systems, Université Libre de Bruxelles (ULB), CP 231, Campus Plaine, 1050 Brussels, Belgium*

[2]*Department of Applied Mathematics, University of Leeds, Leeds, LS2 9JT, United Kingdom*

(Received 30 April 2007; published 10 September 2007)

Traveling fronts can become transversally unstable either because of a diffusive instability arising when the key variables diffuse at sufficiently different rates or because of a buoyancy-driven Rayleigh-Taylor mechanism when the density jump across the front is statically unfavorable. The interaction between such diffusive and buoyancy instabilities of fronts is analyzed theoretically for a simple model system. Linear stability analysis and nonlinear simulations show that their interplay changes considerably the stability properties with regard to the pure Rayleigh-Taylor or diffusive instabilities of fronts. In particular, an instability scenario can arise which triggers convection around statically stable fronts as a result of differential diffusion. Moreover, spatiotemporal chaos can be observed when both buoyancy and diffusive effects cooperate to destabilize the front. Experimental conditions to test our predictions are suggested.

DOI: 10.1103/PhysRevE.76.035301 PACS number(s): 47.20.Bp, 47.55.P−, 47.70.Fw, 82.40.Ck

Propagating fronts are common in nature and can be observed in a wide variety of applications ranging from chemical systems, combustion, biology, and epidemiologic or population systems. They appear typically when an autocatalytic process coupled to diffusion is taking place. The cubic autocatalytic reaction $A+2B \rightarrow 3B$ between a reactant A and autocatalyst B, has been used extensively as a prototype for describing such reaction-diffusion (RD) fronts [1–4]. When the two key species A and B diffuse at similar rates, the front remains planar. If, however, the autocatalyst B diffuses more slowly than the reactant A, the front can lose stability to transverse perturbations [2–4]. It then develops cellular deformations with a wavelength of the order of cm on long diffusive time scales typically of a few hours. This has been observed experimentally using gels soaked with reactants solutions containing also large molecules binding the autocatalyst to slow down its effective diffusivity [5,6]. Traveling fronts can also become unstable through a buoyancy-driven Rayleigh-Taylor (RT) instability when the density of the reactant is different to that of the products across the front [7–17]. If the heavy solution lies on top of the lighter one in the gravity field, a convective fingerlike deformation of the front can then occur on a faster convective time scale of the order of minutes and with a wavelength in the mm range, as is observed experimentally in vertical Hele-Shaw cells [11–15]. By increasing the tilting of the reactor towards the horizontal [13] or increasing uniformly the viscosity of the solution [15], it is possible to slow down the time scale of the RT instability. If the diffusion coefficients of the key variables are such as to allow for a diffusive instability, it could be expected that the convective and diffusive modes act over similar time scales and interact. Previous theoretical work has analyzed diffusive instabilities on the basis of two-variable RD equations in absence of any convection [2–5]. RT fingering of fronts has also been analyzed theoretically on the basis of classical one-variable RD-convection (RDC) models [8–10,16,18] thus excluding the possibility of the differential diffusion effect. Recently, numerical analysis of the influence of differential diffusion on RT fingering has been addressed using a two-variable RDC model but only when the reactant diffuses faster than the autocatalyst, which also excludes diffusive instabilities [17].

In this context, we show here theoretically that the interaction between buoyancy and diffusive instabilities can drastically change the stability and nonlinear properties of a RDC system with respect to the "pure" instabilities considered separately. The coupling between convective and differential diffusive effects can even destabilize an otherwise stable front. Furthermore, when the front features a buoyantly unstable density stratification along with conditions allowing for a diffusive instability, the interplay between the unstable RT and diffusive modes can lead to spatiotemporal chaos. Experimental conditions in which our predictions could be tested are proposed.

Our model consists of a two-dimensional system in which an isothermal RD front resulting from the coupling between the autocatalytic reaction $A+2B \rightarrow 3B$ and diffusion is traveling in the x direction pointing against gravity, y being the transverse coordinate. Initially, ahead of the reaction front A is present, at uniform concentration a_0. It is converted fully into B leaving the product also at a_0. The evolution of the concentrations a and b of species A and B obey RDC equations written, using the standard Boussinesq approximation [10], as

$$\underline{\nabla} \cdot \underline{u} = 0, \quad \underline{\nabla} p = -\frac{\mu}{K}\underline{u} - \rho(a,b) g \underline{e}_x, \tag{1}$$

$$\frac{\partial a}{\partial t} + \underline{u} \cdot \underline{\nabla} a = D_A \nabla^2 a - k_0 a b^2, \tag{2}$$

$$\frac{\partial b}{\partial t} + \underline{u} \cdot \underline{\nabla} b = D_B \nabla^2 b + k_0 a b^2, \tag{3}$$

together with an equation of state $\rho(a,b)=\rho_0+\gamma_1 a+\gamma_2 b$. Here $\rho(a,b)$ is the density of the solution containing the

solutes a and b, ρ_0 is the fluid density of water, and $\gamma_{1,2}$ are the positive solutal expansion coefficients of species A and B. The flow velocity $\underline{u}=(u,v)$ is described by Darcy's law (1) valid in porous media or in thin Hele-Shaw geometries. p denotes the pressure, g is the acceleration of gravity, μ the viscosity, K the permeability, and $\underline{e}_x$ is the unit vector in the x direction. D_A and D_B are the diffusion coefficients of A and B, while k_0 is the kinetic constant.

In absence of flow ($\underline{u}=0$) and for the chosen kinetics, if $D=D_B/D_A<D_c$, with $D_c\simeq 0.424$, the planar RD front becomes diffusionally unstable [2–4]. The front can also become unstable through a RT instability in the presence of an unfavorable density stratification. If the reactants are heavier than the products, $\gamma_1>\gamma_2$ and upward propagating fronts are buoyantly unstable, while fronts propagating downwards remain planar. The reverse is true if $\gamma_1<\gamma_2$ [18].

To analyze the stability of the system in parameter ranges where these two mechanisms generating a transverse instability act on comparable time and length scales, we first nondimensionalize equations (1)–(3) using the characteristic reaction time $T_0=1/k_0a_0^2$, length $L_0=\sqrt{D_AT_0}$, and velocity $U_0=\sqrt{D_A/T_0}$. Density is scaled by $\Delta\rho=(\gamma_1-\gamma_2)a_0$. This leads to the dimensionless equations

$$\nabla^2\psi=-(R_a a_y+R_b b_y), \tag{4}$$

$$a_t+\psi_y a_x-\psi_x a_y=\nabla^2 a-ab^2, \tag{5}$$

$$b_t+\psi_y b_x-\psi_x b_y=D\nabla^2 b+ab^2, \tag{6}$$

where we have introduced the stream function ψ defined by $u=\psi_y$ and $v=-\psi_x$ [10,17] and where the index means derivative with regard to that variable. Here

$$R_{a,b}=\frac{a_0Kg\gamma_{1,2}}{\mu U_0}=\frac{Kg\gamma_{1,2}}{\mu(D_Ak_0)^{1/2}}. \tag{7}$$

If $\gamma_1>\gamma_2$, we have, from Eq. (7), that $R_a>R_b$ and ascending fronts are buoyantly RT unstable. Fronts traveling downwards are convectively unstable if $R_a<R_b$.

Initially $a=1$, $b=0$, and $\psi=0$ (no flow) with a local horizontal input of B to start the reaction. This leads to a pair of counterpropagating RD fronts, which are the base states for a linear stability analysis (LSA). We introduce the traveling coordinate $\zeta=x-ct$, where c is the constant RD front speed, and look for a solution of Eqs. (5) and (6) with $\psi=0$ in the form $a=a(\zeta), b=b(\zeta)$. The traveling front equations in the absence of flow are

$$a_{\zeta\zeta}+ca_\zeta-ab^2=0,\ Db_{\zeta\zeta}+cb_\zeta+ab^2=0 \tag{8}$$

subject, for upward propagating front, to $(a,b)\to(1,0)$ as $\zeta\to\infty$, and $(a,b)\to(0,1)$ as $\zeta\to-\infty$ and conversely for the downward propagating ones. The solution to Eqs. (8) determines the RD front speed c, with c increasing (decreasing) as D is increased (decreased). To consider the stability of the fronts with regard to transverse fluctuations, we perturb this base state by small perturbations of the form $(A,B,\psi)=e^{\sigma t+iky}[A_0(\zeta),B_0(\zeta),\psi_0(\zeta)]$. This leads to an eigenvalue problem for (A_0,B_0,ψ_0) in terms of the growth rate σ and the wavenumber k of the perturbations, subject to $A_0\to 0$, $B_0\to 0, \psi_0\to 0$ as $\zeta\to\pm\infty$.

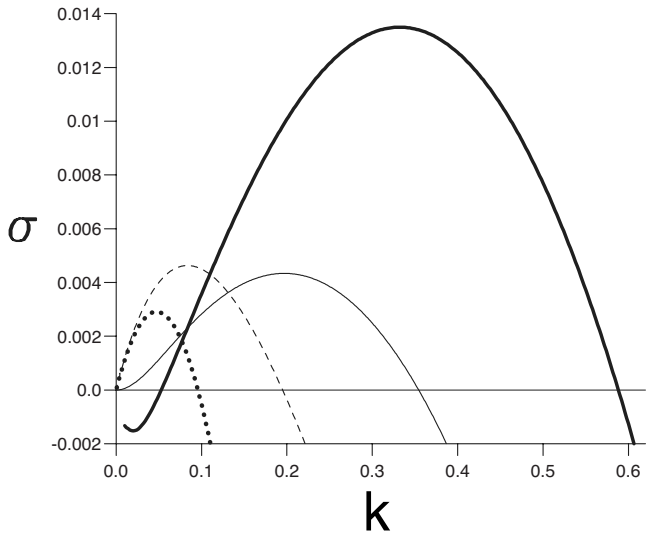

FIG. 1. Dispersion curves for (dotted curve) the RT instability of an ascending front ($R_a=0.5$, $R_b=0.25$, $D=1$); (full curve) the diffusive instability ($R_a=R_b=0$, $D=0.15$); and the mixed case ($R_a=0.5$, $R_b=0.25$, $D=0.15$) for ascending (dashed curve) and descending (bold curve) fronts.

Dispersion curves, plots of σ against k, are obtained for given values of R_a, R_b, and D using standard numerical techniques [4]. Figure 1 shows dispersion curves for the RT and diffusive instabilities and for the case where they interact when $R_a>R_b$. The parameters are chosen so that the growth rates for the two limiting cases are of the same order of magnitude. For $D=1$, ascending fronts where heavier A lies on top of lighter B are buoyantly unstable while descending fronts are stable. If $R_a=R_b=0$ but $D=0.15<D_c$, both fronts are diffusively unstable. Figure 2 presents the corresponding nonlinear cellular deformation of the ascending RT fingered front [Fig. 2(a)] and of the diffusively unstable one [Fig. 2(b)]. These are obtained by numerical integration of Eqs. (4)–(6) using a pseudospectral technique [10,19] with periodic boundary conditions in both directions in a system of dimensionless width $L_y=512$. In the case of the buoyantly induced fingering, convective vortices are at the origin of the transverse deformation and $\psi\neq 0$. Though RT fingering of fronts is known to feature tip splitting in some cases [10,12,14,17], the nonlinear dynamics is characterized for the L_y and small Rayleigh numbers chosen here by a general coarsening trend. This coarsening is captured on Fig. 2(a) by a plot of the extrema of the transverse averaged concentrations [10]. Starting with five fingers the wavelength of which is in agreement with the LSA (see Fig. 1), the RT dynamics feature merging of fingers leading to one final single finger [Fig. 2(a)] [10,14,17]. The descending front for which the density stratification is stable remains planar. The diffusive cellular deformation [Fig. 2(b)] affects both ascending and descending fronts in the same way with a wavelength smaller than for the RT case in agreement with the larger, most unstable wave number predicted by the LSA (Fig. 1). There is no flow in this case ($\psi=0$) and the dynamics are purely diffusive. Chaotic dynamics can result from diffusive insta-

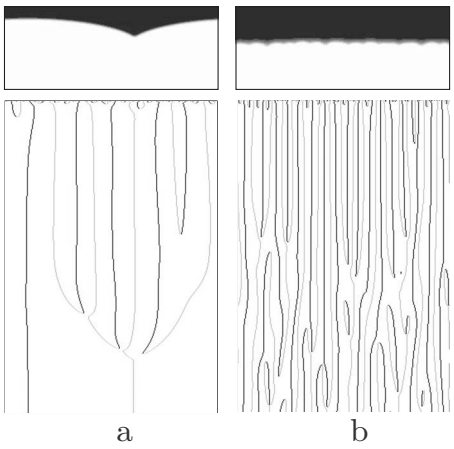

FIG. 2. Nonlinear dynamics of (a) the RT instability (R_a=0.5, R_b=0.25, D=1). Only the upward propagating front is unstable with regard to buoyancy-driven flows ($\psi \neq 0$); (b) the diffusive instability (R_a=R_b=0, D=0.15, ψ=0). The ascending and descending fronts have similar dynamics so we focus here only on the ascending one. On top, a zoom on the deformed front shows the concentration a in a scale ranging from white (a=0, product) to black (a=1, reactant) at time t=7500 in a box of dimensionless width 512 and height 200. The lower panel shows a space-time map of the position of maxima (black) and minima (grey) of transverse averaged profiles from t=0 (top) to t=7500 (bottom).

bilities in large systems and small D [2,3], however, here the nonlinear dynamics are characterized for L_y=512 and D=0.15 by weak interactions between fingers [Fig. 2(b)].

When $R_a > R_b$ and D=0.15, the LSA shows that both ascending and descending fronts are unstable, the latter having the largest growth rate (Fig. 1). Nonlinear simulations confirm these trends: for ascending fronts [Fig. 3(a)], the initial wavelength is smaller (larger most unstable wavenumber in the LSA, see Fig. 1) and the dynamics are characterized by coarsening of fingers in time. For descending fronts, differential diffusion is destabilizing the otherwise buoyantly

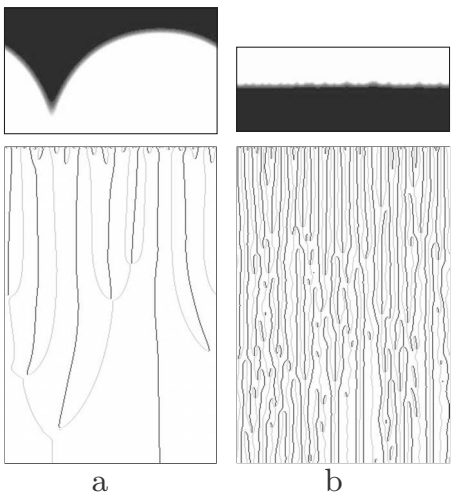

FIG. 3. Same as Fig. 2 with R_a=0.5, R_b=0.25, D=0.15 except that the height of the density plot is here 300 in part (a) and 200 in part (b). Both the upward (a) and downward (b) propagating fronts are deformed by convective flows.

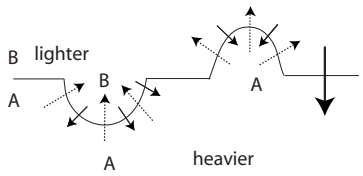

FIG. 4. Displaced particle argument explaining how differential diffusion between the lighter product B and the heavier reactant A can destabilize a downward propagating front featuring a statically stable density stratification. The dotted arrows represent the faster diffusion of A compared to the slower diffusion of B (full arrows). The bold arrow shows the direction of propagation of the front.

stable front which features a smaller wavelength and a more irregular succession of birth and death of fingers in the nonlinear regime [Fig. 3(b)]. To understand this, consider the displaced particle argument shown in Fig. 4 for the downward propagating front. A perturbation ahead of the front fills in faster with heavier A than losing lighter B when $D_B < D_A$. Thus the perturbation becomes heavier than the surrounding fluid containing only A and hence continues to sink driving an instability of the otherwise buoyantly stable density stratification. Similarly, a perturbation behind the front loses heavier A by diffusion more than gaining lighter B, hence the perturbation is lighter than its surroundings and

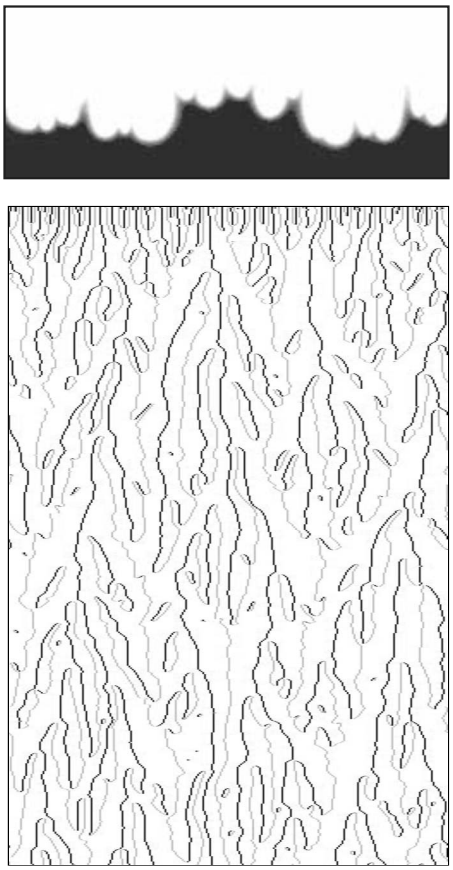

FIG. 5. Same as Fig. 2 with R_a=0.25, R_b=0.5, D=0.15. Only the downward propagating front is unstable. The system features complex dynamics due to the interaction of RT and diffusive instabilities, which are both destabilizing.

can rise. This mechanism is related to solutal double-diffusive effects [20,21] with, however, the dynamics being influenced by the diffusive instability when $\Delta\rho \to 0$. It is reinforced by the fact that the RD speed c decreases with D, which favors the development of buoyant flows.

For upward moving fronts, a similar displaced particle argument predicts a stabilizing effect of differential diffusion on the RT instability while the slower RD speed c when D decreases, on the contrary, favors it. These competing effects lead to a nonmonotonous dependence of the most unstable growth rate when D is lowered below 1. The fact that $D_B < D_A$ is thus having a complex influence on the RT unstable ascending front and is able to trigger convection around a descending front that is buoyantly stable for $D=1$. Arguing along similar lines shows that, if $R_a < R_b$, i.e., the product B is now heavier than the reactant A, the fact that $D_B < D_A$ will on the contrary reinforce the stability of buoyantly stable ascending fronts and the instability of RT unstable descending fronts. This is fully borne out by linear stability calculations performed for $R_a < R_b$ and $D=0.15$. Negative growth rates are obtained for ascending fronts, while enhanced destabilization with regard to the pure diffusive dispersion curve is obtained for descending fronts. Figure 5 shows that, in the nonlinear regime, this interplay between both destabilizing RT and diffusive modes results in spatiotemporal chaotic dynamics characterized by complex interactions, merging, and tip spitting of fingers.

In summary, we have shown theoretically that the interplay between diffusive and RT instabilities of fronts can affect the stability and nonlinear properties of the system. A convective instability of a statically stable descending front can be induced if the two components diffuse at different rates. Spatiotemporal chaos of descending fronts is obtained when convective and diffusive modes are both destabilizing. Experimental demonstration of the predicted instability scenarios and dynamics could be tested using, for example, the autocatalytic iodate arsenous acid [5,11,12] or the chlorite-tetrathionate [6,13,14] reactions. Both reactions have been used in the past to study separately cellular deformations due to diffusive instabilities in gels [5,6] or RT fingering in vertical Hele-Shaw cells [11–15,18]. We now propose to analyze their dynamics in the presence of the large molecules binding the activator used in Refs. [5,6] to obtain $D < D_c$. The dynamics should, however, be studied not in gels but in aqueous solutions contained in Hele-Shaw cells slightly inclined to the horizontal or containing a chemically inert viscous solute. This would slow down the buoyant flows to bring their characteristic time scales down to those necessary for them to interact with the diffusive modes.

J.D. acknowledges support from the FRIA. A.D. thanks ESA, Prodex, FNRS, and the Communauté française de Belgique for financial support.

[1] A. Hanna, A. Saul, and K. Showalter, J. Am. Chem. Soc. **104**, 3838 (1982).
[2] D. Horváth *et al.*, J. Chem. Phys. **98**, 6332 (1993).
[3] A. Malevanets, A. Careta, and R. Kapral, Phys. Rev. E **52**, 4724 (1995).
[4] J. H. Merkin and I. Z. Kiss, Phys. Rev. E **72**, 026219 (2005).
[5] D. Horváth and K. Showalter, J. Chem. Phys. **102**, 2471 (1995).
[6] A. Tóth, I. Lagzi, and D. Horváth, J. Phys. Chem. **100**, 14837 (1996).
[7] J. A. Pojman *et al.*, J. Phys. Chem. **95**, 1299 (1991).
[8] D. A. Vasquez, J. W. Wilder, and B. F. Edwards, J. Chem. Phys. **98**, 2138 (1993).
[9] A. De Wit, Phys. Rev. Lett. **87**, 054502 (2001).
[10] A. De Wit, Phys. Fluids **16**, 163 (2004).
[11] M. Böckmann and S. C. Müller, Phys. Rev. Lett. **85**, 2506 (2000).
[12] M. Böckmann and S. C. Müller, Phys. Rev. E **70**, 046302 (2004).
[13] D. Horváth, T. Bánsági, Jr., and A. Tóth, J. Chem. Phys. **117**, 4399 (2002).
[14] T. Bánsági, Jr., D. Horváth, and A. Tóth, J. Chem. Phys. **121**, 11912 (2004).
[15] T. Rica, D. Horváth, and A. Tóth, Chem. Phys. Lett. **408**, 422 (2005).
[16] N. Vladimirova and R. Rosner, Phys. Rev. E **67**, 066305 (2003).
[17] J. Yang *et al.*, J. Chem. Phys. **117**, 9395 (2002); D. Lima *et al.*, *ibid.* **124**, 014509 (2006).
[18] J. D'Hernoncourt, A. Zebib, and A. De Wit, Phys. Rev. Lett. **96**, 154501 (2006); Chaos **17**, 013109 (2007).
[19] C. T. Tan and G. M. Homsy, Phys. Fluids **31**, 1330 (1988).
[20] I. P. Nagy *et al.*, J. Phys. Chem. **98**, 6030 (1994); A. Kereszttessy *et al.*, *ibid.* **99**, 5379 (1995).
[21] S. E. Pringle and R. J. Glass, J. Fluid Mech. **462**, 161 (2002).